

Supporting Information

Surface conversion of CuO-ZnO to ZIF-8 to enhance CO₂ adsorption for CO₂ hydrogenation to methanol

Lei Zhang^a, Jia Cui^a, Yue Zhang^a, Xiaoguang San^{a*}, Dan Meng^{a*}

^a College of Chemical Engineering, Shenyang University of Chemical Technology, Shenyang 110142, PR China

*Corresponding authors. Tel./fax: +86 136-5401-9351

Email: sanxiaoguang@syuct.edu.cn (X. San); mengdan0610@hotmail.com (D. Meng)

Contents

Fig. S1. FTIR spectra of co-precipitated CuO-ZnO, hydrothermal CuO-ZnO and CuO-ZnO@ZIF-8.

Fig. S2. Low-magnification and high-magnification SEM of image (a) CuO-ZnO@ZIF-8(1:2), (b) CuO-ZnO@ZIF-8(1:4) and (c) CuO-ZnO@ZIF-8(1:6).

Fig. S3. HRTEM images of CuO-ZnO@ZIF-8 (1:4).

Fig. S4. Raman spectra of co-precipitated CuO-ZnO, hydrothermal CuO-ZnO and CuO-ZnO@ZIF-8(1:4).

Fig. S5. XPS spectra of CuO-ZnO@ZIF-8(1:4) catalysts: (a) survey XPS spectra of CuO-ZnO@ZIF-8 (b) Zn 2p (c) C 1s(d) N 1s (e) O 1s and (f) Cu 2p.

Fig. S6. TG diagrams (a) and TPR patterns (b) of co-precipitated CuO-ZnO, hydrothermal CuO-ZnO and CuO-ZnO@ZIF-8 catalysts.

Fig. S7. XRD pattern of co-precipitated CuO-ZnO, hydrothermal CuO-ZnO and CuO-ZnO@ZIF-8 after reaction.

Fig. S8. MS spectra of the CO₂ reduction products of CuO-ZnO@ZIF-8 using ¹²CO₂ and ¹³CO₂.

Tab. S1. FTIR spectra of the absorption CO₂ (g) features in ZnO and CuO nanoparticle Surface.

Tab. S2. The oxygen vacancies relative concentration ratios by XPS (%).

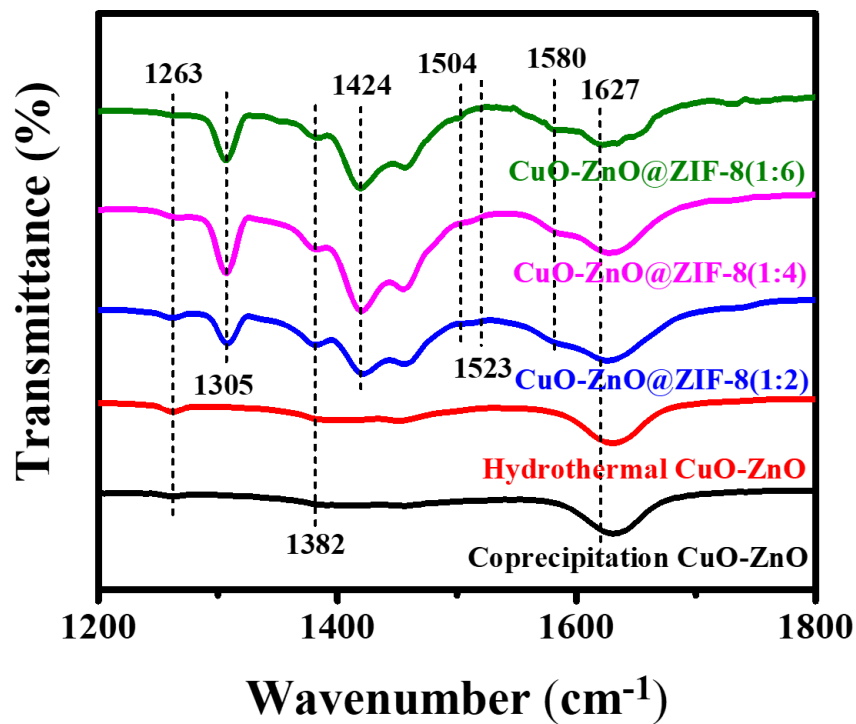


Fig. S1. FTIR spectra of co-precipitated CuO-ZnO, hydrothermal CuO-ZnO and CuO-ZnO@ZIF-8.

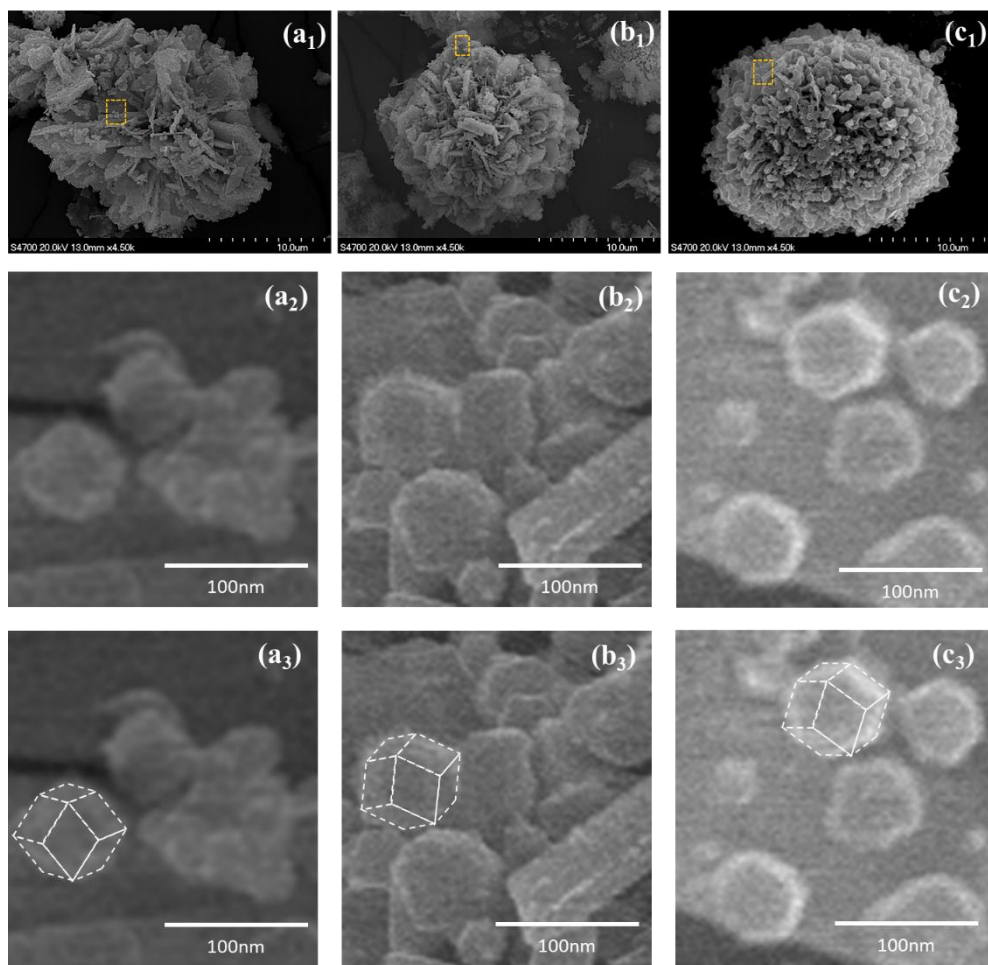


Fig. S2. Low-magnification and high-magnification SEM of image (a) CuO-ZnO@ZIF-8(1:2), (b) CuO-ZnO@ZIF-8(1:4) and (c) CuO-ZnO@ZIF-8(1:6).

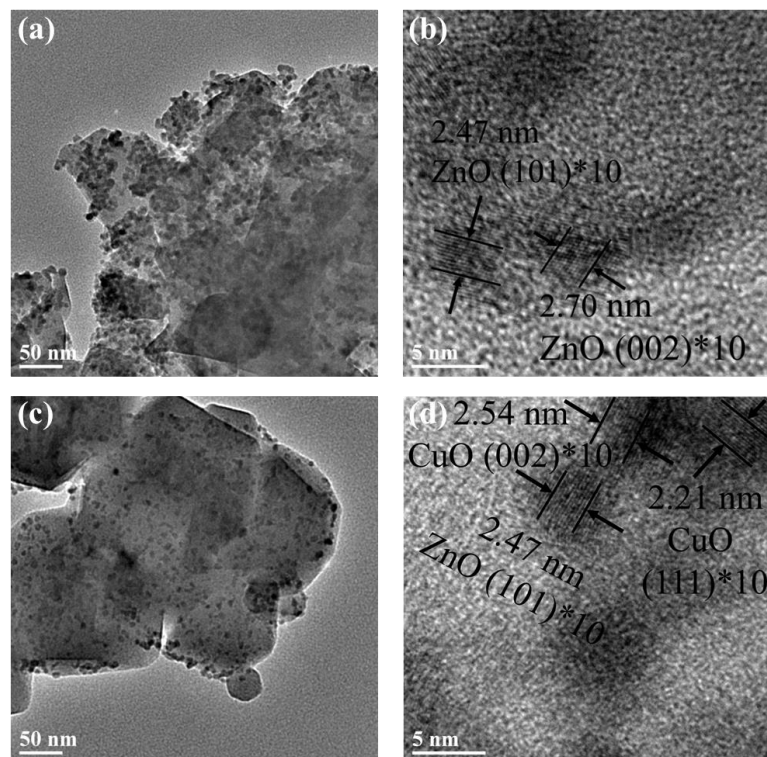


Fig. S3. HRTEM images of CuO-ZnO@ZIF-8 (1:4).

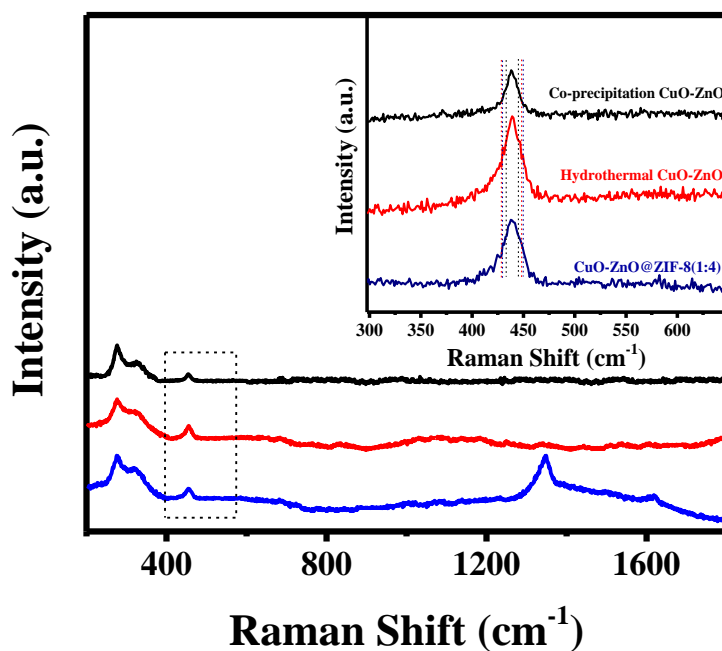


Fig. S4. Raman spectra of co-precipitated CuO-ZnO, hydrothermal CuO-ZnO and CuO-ZnO@ZIF-8(1:4).

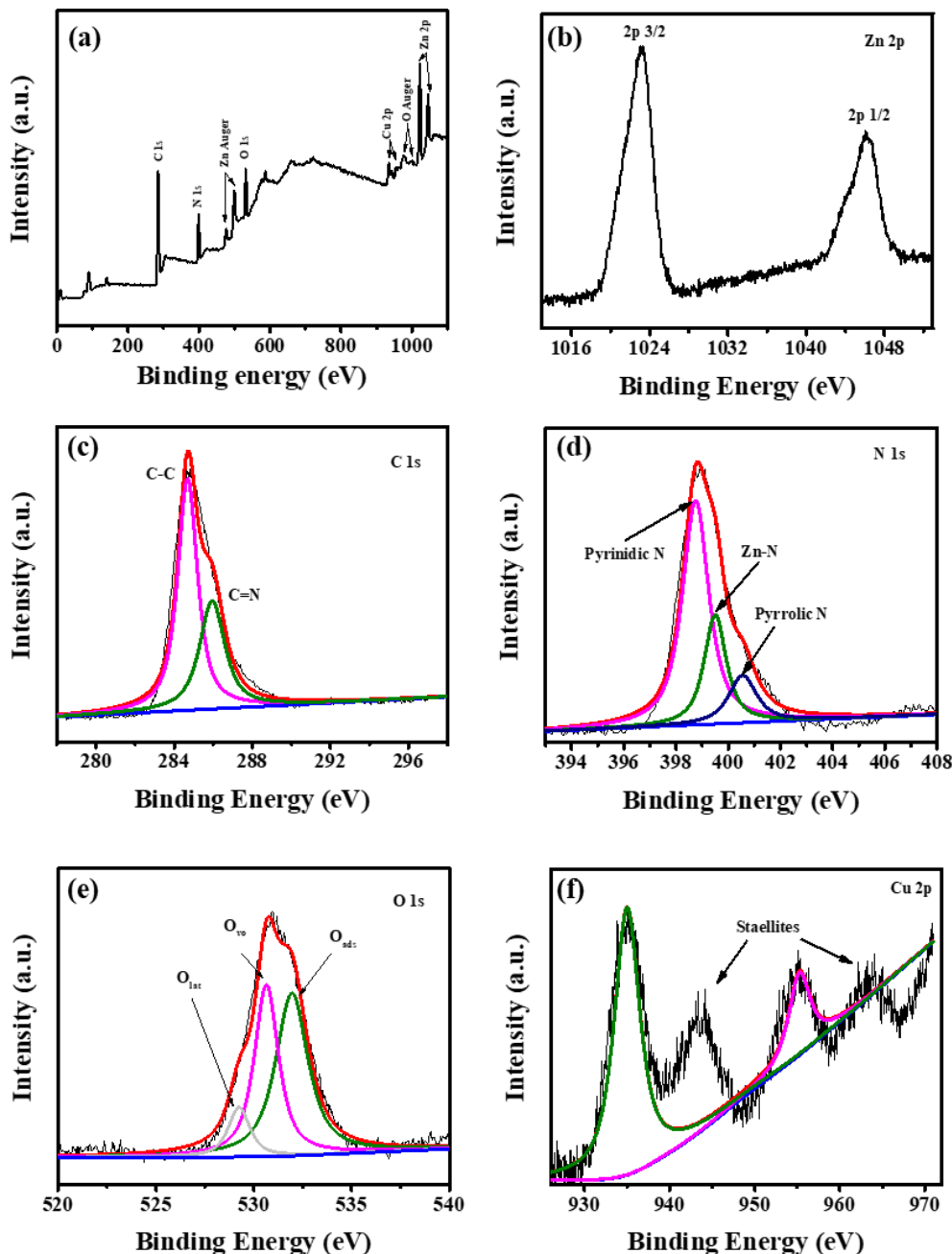


Fig. S5. XPS spectra of CuO-ZnO@ZIF-8(1:4) catalysts: (a) survey XPS spectra of CuO-ZnO@ZIF-8 (b) Zn 2p (c) C 1s(d) N 1s (e) O 1s and (f) Cu 2p.

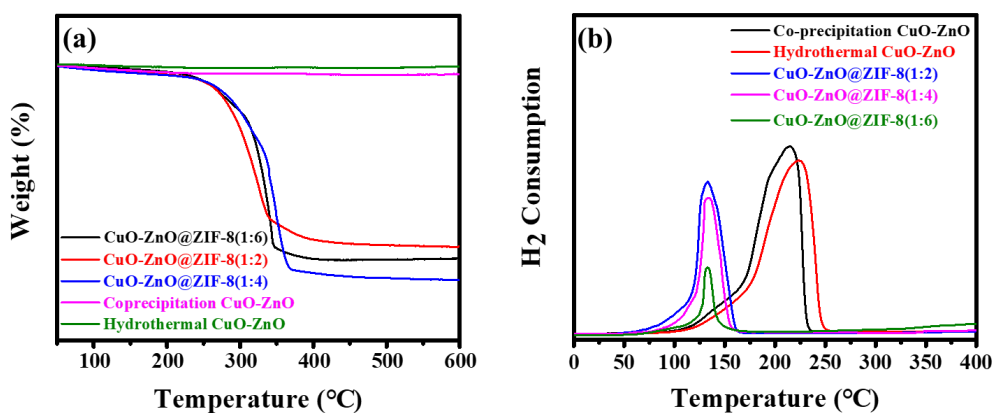


Fig. S6. TG diagrams (a) and TPR patterns (b) of co-precipitated CuO-ZnO, hydrothermal CuO-ZnO and CuO-ZnO@ZIF-8 catalysts.

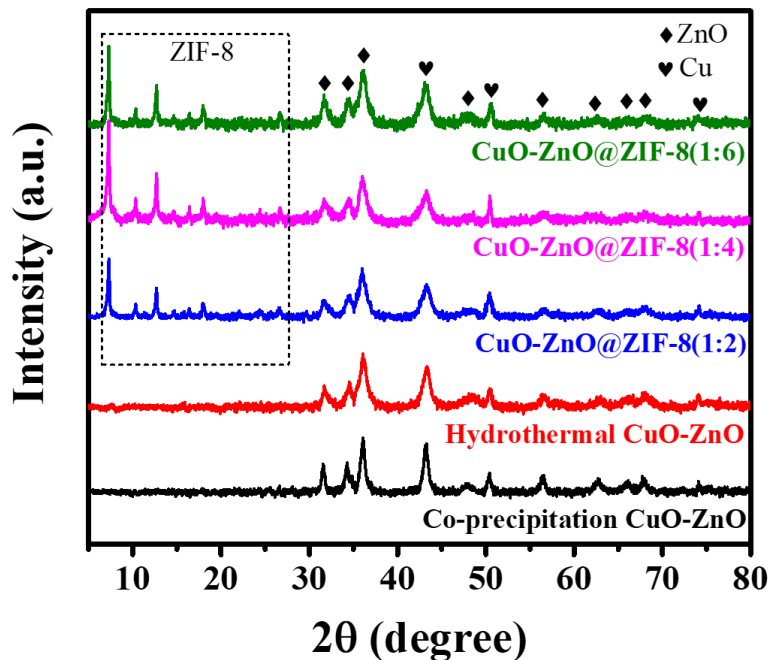


Fig. S7. XRD pattern of co-precipitated CuO-ZnO, hydrothermal CuO-ZnO and CuO-ZnO@ZIF-8 after reaction.

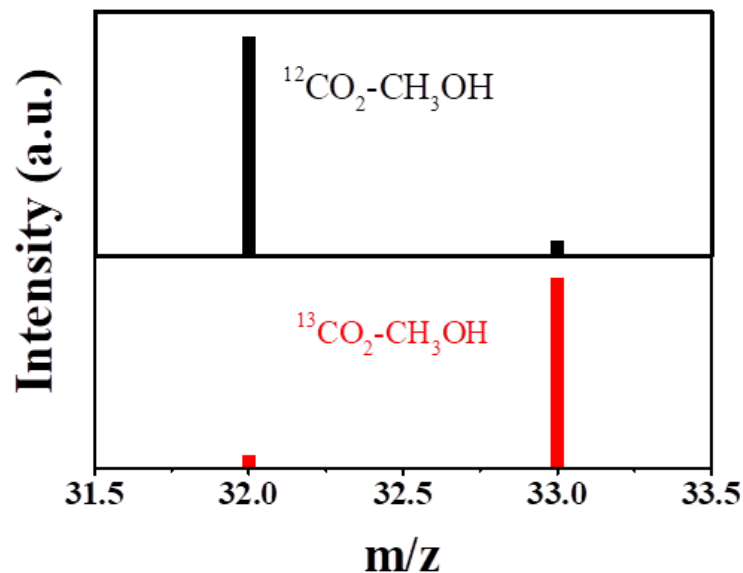


Fig. S8. MS spectra of the CO_2 reduction products of CuO-ZnO@ZIF-8 using $^{12}\text{CO}_2$ and $^{13}\text{CO}_2$.

Tab. S1.

FTIR spectra of the absorption CO₂ (g) features in ZnO and CuO nanoparticle Surface.

Vibrational Assignment	Bicarbonate				Monodentate carbonate				Bidentate carbonate				Carboxylate	
	v_3 (O-C-O) _{as}		v_3 (O-C-O) _s		v_3 (O-C-O) _{as}		v_3 (O-C-O) _s		v_3 (O-C-O) _{as}		v_3 (O-C-O) _s		v_3 (O-C-O) _{as}	
	ZnO (cm ⁻¹)	CuO (cm ⁻¹)	ZnO (cm ⁻¹)	CuO (cm ⁻¹)	ZnO (cm ⁻¹)	CuO (cm ⁻¹)	ZnO (cm ⁻¹)	CuO (cm ⁻¹)	ZnO (cm ⁻¹)	CuO (cm ⁻¹)	ZnO (cm ⁻¹)	CuO (cm ⁻¹)	ZnO (cm ⁻¹)	ZnO (cm ⁻¹)
CuO-ZnO@ZIF-8(1:6)	1627	—	—	1424	1504	—	1382	—	1580	—	1263	1305	1523	—
CuO-ZnO@ZIF-8(1:4)	1627	—	—	1424	1504	—	1382	—	1580	—	1263	1305	1523	—
CuO-ZnO@ZIF-8(1:2)	1627	—	—	1424	1504	—	1382	—	1580	—	1263	1305	1523	—
Hydrothermal CuO-ZnO	1631	—	—	—	—	—	1386	—	—	—	1263	—	—	—
Coprecipitation CuO-ZnO	1631	—	—	—	—	—	1386	—	—	—	1263	—	—	—
Range of Frequencies (cm ⁻¹ ^{a-e})	1623-1650 ^a	1410-1435 ^a	1480-1520 ^{a-c}	1380-1395 ^a	1553-1644 ^{a,b}	1243-1355 ^{a,b}	1510-1670 ^{a,c,d}							

a. Ref 1; b. Ref, 2; c. Ref. 3 d. Ref. 4; e. Ref. 5

Tab. S2.

The oxygen vacancies relative concentration ratios by XPS (%).

Catalyst	O _{vo} /(O _{lat} + O _{vo} + O _{ads})
Co-precipitation Cu-ZnO	21
Hydrothermal CuO-ZnO	35
CuO-ZnO@ZIF-8 (1:4)	39

References

- 1 Baltrusaitis, J.; Shuttlefield, J.; Zeitler, E.; Grassian, V. H. Carbon Dioxide Adsorption on Oxide Nanoparticle Surfaces. *Chem. Engine, J.* **2011**, *170*, 471-481.
- 2 Noei, H.; Woll, C.; Muhler, M.; Wang, Y. Activation of Carbon Dioxide on ZnO Nanoparticles Studied by Vibrational Spectroscopy. *J. Phys. Chem. C* **2011**, *115*, 908-914.
- 3 Shido, T.; Iwasawa, Y. Reactant-Promoted Reaction Mechanism for Water-Gas Shift Reaction on Rh-Doped CeO₂. *J. Catal.* **1993**, *141*, 71-81.
- 4 Seiferth, O.; Wolter, K.; Dillmann, B.; Klivenyi, G.; Freund, H.-J.; Scarano, D.; Zecchina, A. IR Investigations of CO₂ Adsorption on Chromia Surfaces: Cr₂O₃ (0001)/Cr (110) versus Polycrystalline α -Cr₂O₃. *Surf. Sci.* **1999**, *421*, 176-190.
- 5 Baltrusaitis, J.; Jensen, J. H.; Grassian, V. H. FTIR Spectroscopy Combined with Isotope Labeling and Quantum Chemical Calculations to Investigate Adsorbed Bicarbonate Formation Following Reaction of Carbon Dioxide with Surface Hydroxyl Groups on Fe₂O₃ and Al₂O₃. *J. Phys. Chem. B* **2006**, *110*, 12005-12016.